11TH INTERNATIONAL CONFERENCE ON HAND-ARM VIBRATION

AN INVESTIGATION ON THE BIODYNAMIC FOUNDATION OF A RAT TAIL VIBRATION MODEL

Daniel E. Welcome, Kristine Krajnak, Ren G. Dong

Health Effects Laboratory Division, National Institute for Occupational Safety and Health, Morgantown, WV (USA)

Abstract

The rat tail model has been used to examine the mechanisms of vibration-induced finger disorders. To help clarify whether the tail model can provide a good simulation of finger vibration exposure, this study investigated the biodynamic foundation of the rat tail model using a mechanical-equivalent model established based on the vibration transmissibility measured on the rat tail. The mechanical model was used to estimate the natural frequency, damping, dynamic deformation and vibration power absorption intensity of the rat tail, which is directly associated with the dynamic stresses/strains inside the rat tail. The rat tail vibration power absorption intensity was compared with those of the fingers that were estimated from a reported hand-arm system mechanical model. This study found that the basic trend of the rat tail biodynamic response in the frequency domain different from that of the human fingers. This suggests that the frequency dependencies of their biological effects may not be directly comparable. However, knowledge of the rat tail biodynamic responses may be used to examine the relationship between biodynamics and health effects.

1. Introduction

Laboratory studies in humans have demonstrated that the transmission of vibration from a hand tool to the body is frequency dependent, and that the dependencies are different in the arms, hands and fingers [1-4]. The first dominant resonance of the overall hand-arm system is in the range of 25 to 50 Hz. The vibration transmissibility at the fingers can remain at a high level up to 500 Hz, with a resonant frequency in the range of 80 to 300 Hz [3, 4] mainly depending on the applied finger force and vibration direction [1]. Epidemiological studies have also found that the prevalence of hand-arm vibration syndrome (HAVS) is highest in workers exposed to hand tools that produce dominant vibrations in the mid-range frequencies (i.e., 25 to 500 Hz) [5-7]. These laboratory and epidemiological findings have lead to the formulation of the hypothesis that vibration exposures that result in greater biodynamic response increase the risk of developing a disorder. However, it is very difficult to conduct biological studies to directly test this hypothesis in humans.

Animal models have been developed and utilized to describe the soft tissue damage that can be induced by exposure to vibration. Models exposing rat hind limbs or tails to chronic vibration (200-800 hrs) have demonstrated that repeated exposures to vibration result in damage to vascular, neural and muscle tissues [8-12], and that the damage is similar to that seen in biopsy tissues collected from workers diagnosed with HAVS [13, 14]. However, the majority of these animal studies exclusively used lower frequency vibration exposures (e.g. $\leq$ 60 Hz) [8-12]. The effects of repeated exposures to vibration in the higher mid-range frequencies (100-300 Hz) have been far from sufficiently examined in animal models. Studies of the effects on rat models from single bouts of vibration have also suggested that the responses of neural and vascular tissues are frequency dependent [15, 16].

It remains unclear whether the rat tail model can provide a reasonable simulation of the finger vibration exposure. It is also unclear whether the frequency-dependencies and dose-response relationships that can be identified from this animal model can be directly applied to predict the finger disorders. To help clarify these issues, it is very important to compare the essential mechanical stimuli (stresses/strains) that are directly acting on the cells and tissues of the finger and rat-tail [17]. This study investigated the biodynamic foundation of the rat tail model using a mechanical-equivalent model established based on the vibration transmissibility measured on the rat tail. The mechanical model was used to estimate the dynamic deformation of the rat tail, which is directly associated with the dynamic stresses/strains inside the rat tail. The rat tail dynamic deformation was used to calculate the vibration power absorption intensity which was compared with those of the fingers that were estimated from a reported hand-arm system mechanical model.

2. Methods

2.1 Mechanical Equivalent Models

Figure 1a illustrates a model of human hand-arm system with hand gripping on a cylindrical handle, which was recently developed by Dong et al. [18]. The fingers are simulated using two degrees of freedom (DOFs): M_2 is the finger effective mass and M_4 is the contact skin effective mass. Such a model provided a reasonable simulation of the biodynamic responses of the fingers in terms of both mechanical impedance and vibration transmissibility [18]. Therefore, this model was used in this study for evaluating the rat tail model. Similar to the finger model, the rat-tail was also modelled using two DOFs, as shown in figure 1b. These models make it possible to estimate the natural frequency, damping ratio, effective vibration deformation, and vibration power absorption intensity (VPAI) of the fingers and the rat tail.

2.2 Transmissibility Measurement

Whereas the parameters of the hand-arm system model are available [18] and they were directly used in this study, the parameters of the rat tail model were determined using the vibration transmissibility of the rat tail. The transmissibility values on the tails of four male Sprague Dawley rats (6 weeks of age; Hilltop Lab Animals, Inc, Scottsdale, PA) were measured. The tails were gently elastically strapped to an elliptically shaped plate attached to an electromagnetic shaker (Ling Dynamics V408) as shown in figure 2. A scanning laser vibrometer (Polytec, PSV-300-H) was used to measure the vibration at each of 13 points along the tail as compared to that at the plate. Three accelerations (1g, 5g, and 10g) at six different frequencies (32, 63, 125, 160, 250, 500 Hz) were used in the vibration exposure. A three-factor-repeated-measures analysis of variance was used to conduct the general statistical analysis using index point location, vibration frequency, and vibration magnitude as the factors with animal as a fixed effect.

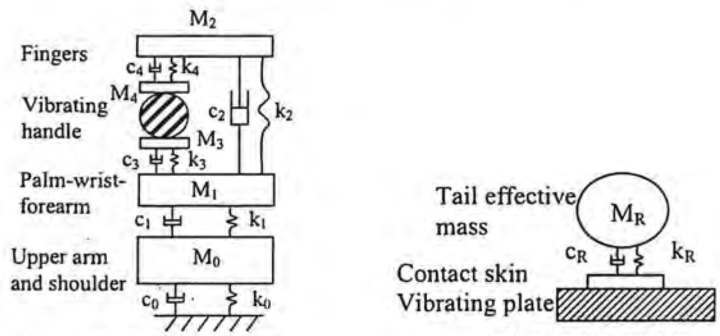

(a) Human hand-arm model (b) Rat-tail model

Figure 1 - Mechanical equivalent models of the human hand-arm system and the rat tail

Figure 2 - Map of index points

2.3 Calculation of VPA Intensity

In the fingers-hand-arm system model shown in figure 1a, the fingers are represented using two masses ($M_{Fingers}$ and M_{Skin}) coupled through linear stiffness ($k_{Fingers}$) and viscous damping ($c_{Fingers}$) due to finger tissues. Mass M_{Skin} represents effective mass of the finger skin contacting the handle. Mass $M_{Fingers}$ is effective mass due to finger tissues and bones. The relative displacement ($\Delta D_{Fingers}$) between masses $M_{Fingers}$ and M_{Skin} was used to represent the overall deformation of the fingers. The energy dissipated by viscous element $c_{Fingers}$, which is directly related to the relative displacement, is used to represent the power ($P_{Fingers}$) absorbed within fingers tissues. Specifically, it is calculated from:

$$P_{Fingers}(\omega) = c_{Fingers}\left[\omega \cdot \Delta D_{Fingers}(\omega)\right]^2 \tag{1}$$

In the rat tail model shown in figure 1b, the moving effective mass (M_{Tail}) in the mechanical model was assumed to be the tail mass per unit length. To determine this effective mass at each measuring location, the mass and length of each tested tail, as well as the cross-sectional areas of the tail at three locations (C, G, and K) were measured, and a conical shape of the tail was assumed. The other mass, skin mass, considered in the model has little effect on the determinations of resonant frequency, damping ratio and dynamic deformation required in this study. Therefore, it is not determined in this study. As the first degree of approximation, a linear effective contact stiffness (k_{Tail}) and viscous damping (per unit length) (c_{Tail}) were assumed. The shear stiffness or the interaction along the length of the tail was ignored. Therefore, the mechanical rat tail model is effectively a one-DOF model. The measured vibration transmissibility was used to determine the stiffness and damping of the rat tail model using a least root-mean-square (rms) method: minimizing the rms difference between the modelling prediction and the measured transmissibility data. Once the model parameters for the tail model at each location are determined, the relative displacement (ΔD_{Tail}) between tail equivalent mass and the vibrating plate was calculated and used to represent the overall deformation of the tail. With the deformation, the power absorbed by the tail at that location (P_{Tail}) can be calculated from:

$$P_{Tail}(\omega) = c_{Tail}\left[\omega \cdot \Delta D_{Tail}(\omega)\right]^2 \tag{2}$$

P_{Tail} and $P_{Fingers}$ are not directly comparable because P_{Tail} represents the VPA per unit tail length but $P_{Fingers}$ is the total VPA of the fingers. To compare their frequency dependencies, their VPA values at a specific frequency are not critical but the shapes of their VPA functions in the frequency domain are of concern. For this reason, each VPA function is normalized by dividing its corresponding critical damping value and taking a square root of the resulting function. The normalized function is called VPA intensity (VPAI) function in this study. It is a linear function of the input vibration (displacement, velocity, or acceleration) and expressed as follows:

$$VPAI_{Tail}(\omega) = \omega \cdot \Delta D_{Tail}(\omega) \cdot \sqrt{\xi_{Tail}} \tag{3}$$

$$VPAI_{Fingers}(\omega) = \omega \cdot \Delta D_{Fingers}(\omega) \cdot \sqrt{\xi_{Fingers}} \quad (4)$$

In such a way, the two energy measures are directly comparable.

3. Results and Discussion

The transmissibility was significantly influenced by the location x frequency x magnitude interaction ($p<.0001$). Points C, D, E, F, G, and K all showed significant responses by frequency ($p<.001$), while C, D, E, G, and K showed a significant frequency x magnitude interaction ($p<.05$). Therefore only those 6 points were modelled and presented in figure 3. Points D, E, G, and K were not constrained by the straps and responded with less damping than C and F. The resonant frequency range was between 160 and 370 Hz, decreasing by location along the length of the tail and with increasing vibration input magnitude. Table 1 summarizes the system parameters determined through the models.

As an example, figure 4 shows the comparison of the finger and rat-tail vibration power absorption intensities. The acceleration in the example is 5g-rms at each measurement point for the rat tail, while the influence of coupling at multiple input magnitudes was modelled for the human fingers in figure 4b. The first resonant peak (at about 40 Hz) of the fingers is due to the resonance of the entire hand-arm system that is mainly determined from the palm contact stiffness and the effective mass of the entire hand-arm system [18]. The rat tail has no such resonance. The second resonance of the finger response is at about 260 Hz, which is independent of the remaining hand-arm system [18]. The rat tail resonant frequency is comparable with this finger resonant frequency. Because the rat tail generally has a lower damping ratio than the fingers, the tail has higher VPA intensity in this resonant frequency range. Therefore, the overall shapes of their VPA intensities expressed in the frequency domain are inconsistent.

Table 1 - Summary of natural frequencies and damping ratios of the rat tail at six typical locations

Measuring location	C			D			E		
Vibration input (g)	1	5	10	1	5g	10g	1g	5g	10g
Natural frequency (Hz)	368	278	193	319	235	212	324	241	221
Damping ratio	0.366	0.692	0.721	0.094	0.202	0.219	0.147	0.236	0.253
Measuring location	F			G			K		
Vibration input (g)	1	5	10	1	5g	10g	1g	5g	10g
Natural frequency (Hz)	245	224	172	223	198	161	233	208	201
Damping ratio	0.523	0.580	0.872	0.174	0.202	0.394	0.170	0.224	0.365

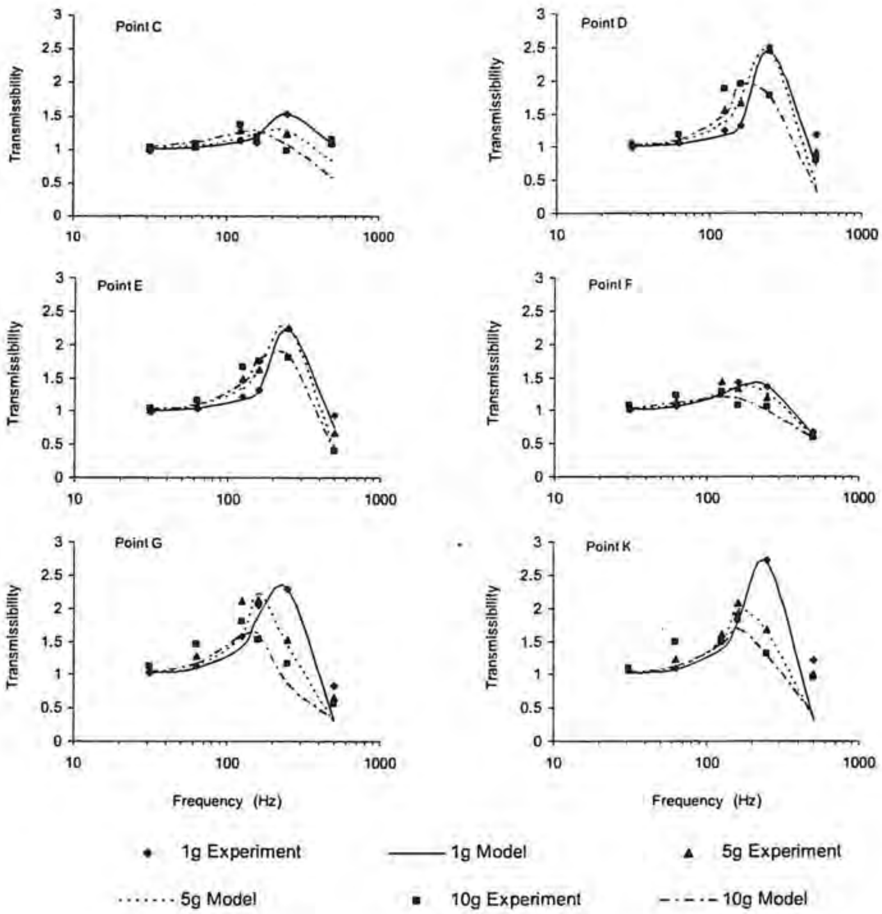

Figure 3 - Modelled and measured transmissibility for each input magnitude at each point with a significant frequency response

These observations suggest that although the natural frequency of the rat tail is similar to that of human fingers, the damping and the vibration power absorption intensity of the rat tail are different from those of the fingers. The higher resonant intensity of the rat tail suggests that the rat tail model may be an accelerated model for studying the vibration-induced disorders of human fingers. Furthermore, the rat tail model may also be used to examine the relationship between the biodynamic response and the health effects.

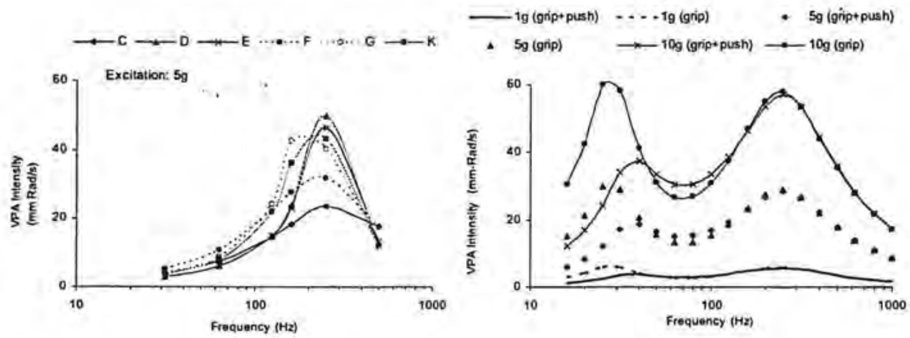

(a) (b)

Figure 4 - Vibration power absorption intensity calculated (a) for the rat tail at an excitation of 5g for each of the significant measurement points, and (b) for the human fingers using the models reported in Dong et al. [18]

4. Conclusions

This study found that the basic trend of the rat tail biodynamic response in the frequency domain different from that of the human fingers. This suggests that the frequency dependencies of their biological effects may not be directly comparable. However, knowledge of the rat tail biodynamic responses may be used to examine the relationship between biodynamics and health effects.

References

[1] R.G. Dong, T.W. McDowell, D.E. Welcome, J.Z.Wu, Biodynamic response of human fingers in a power grip subjected to a random vibration. Journal of Biomechanical Engineering **126**, 446-456 (2004)

[2] Kihlberg S, Biodynamic response of the hand-arm system to vibration from an impact hammer and a grinder. International Journal of Industrial Ergonomics **16**, 1-8 (1995)

[3] D. Reynolds, E.N. Angevine, Hand-arm vibration, part II: Vibration transmission characteristics of the hand and arm. Journal of Sound Vibration **51**, 255-265 (1977).

[4] A. Sörensson, R. Lundström. Transmission of vibration to the hand. Journal of Low Frequency Noise and Vibration **11**, 14-22 (1992)

[5] M.J. Griffin, Handbook of Human Vibration. San Diego, Academic Press, 1990.

[6] M. Bovenzi, Exposure-response relationship in the hand-arm vibration syndrome: an overview of current epidemiology research. International Archives of Occupational & Environmental Health **71**, 509-19 (1998)

[7] M. Bovenzi, A. Franzinelli, F. Strambi, Prevalence of vibration-induced white finger and assessment of vibration exposure among travertine workers in Italy. Int Arch Occup Environ Health **61**, 25-34 (1988)

[8] A.J. Brammer, I. Pyykko, Vibration-induced neuropathy. Detection by nerve conduction measurements. Scand J Work Environ Health, **13**, 317-22 (1987)

[9] K.Y. Chang, S.T. Ho, H.S.Yu, Vibration induced neurophysiological and electron microscopic changes in rat peripheral nerves. Occupational & Environmental Medicine, **51**, 130-5 (1994)

[10] B.D. Curry, J.L. Bain, J.G. Yan, L.L. Zhang, M. Yamaguchi, H.S. Matloub, et al. Vibration injury damages arterial endothelial cells. Muscle & Nerve **25**, 527-34 (2002)

[11] B. Hellstrom, Effects of local vibration on the rat tail circulation. Internationales Archiv fur Arbeitsmedizin, **33**, 285-95 (1974)

[12] L.E. Necking, L.B. Dahlin, J. Friden, G. Lundborg, R. Lundstrom, L.E., Thornell Vibration-induced muscle injury. An experimental model and preliminary findings. J Hand Surg [Br], **17**, 270-4 (1992)

[13] T. Takeuchi, M. Futatsuka, H. Imanishi, S. Yamada, Pathological changes observed in the finger biopsy of patients with vibration-induced white finger. Scand J Work Environ Health **12**, 280-3 (1986)

[14] T. Takeuchi, M. Takeya, H. Imanishi, Ultrastructural changes in peripheral nerves of the fingers of three vibration-exposed persons with Raynaud's phenomenon. Scand J Work Environ Health **14**, 31-5 (1988)

[15] A. Okada, Physiological response of the rat to different vibration frequencies. Scandinavian Journal of Work, Environment & Health, **12**, 362-4 (1986)

[16] B.D. Curry, S. Govindaraju, J.L.W. Bain, L.L. Zhang, J-G. Yan, H.S. Matloub, et al. Evidence for frequency-dependent arterial damage in vibrated rat tails. In: 38th United Kingdom Conference on Human Response to Vibration; Institute of Naval Medicine, Alverstoke, Gosport, England; p. 179-196 (2003)

[17] R.G. Dong, J.Z. Wu, D.E. Welcome, Recent advances in biodynamics of hand-arm system. Industrial Health **43**, 449-471 (2005)

[18] R.G. Dong, J.H. Dong, J.Z. Wu, and S. Rakheja, "Modelling of biodynamic responses distributed at the fingers and the palm of the human hand-arm system", Journal of Biomechanics (in press. Available on-line since December 2006).

Disclaimer

The findings and conclusions in this paper have not been formally disseminated by the National Institute for Occupational Safety and Health and should not be construed to represent any agency determination or policy.

11TH INTERNATIONAL CONFERENCE ON HAND-ARM VIBRATION

ASSOCIAZIONE ITALIANA di ACUSTICA

ISPESL
Istituto Superiore per la Prevenzione e la Sicurezza del Lavoro

We are pleased to welcome you on the CD-ROM Proceedings of the *Eleventh International Conference on Hand-Arm Vibration*

Bologna, Italy
3-7 June 2007

Proceedings edited by

M. Bovenzi, A. Peretti,
P. Nataletti, G. Moschioni